Atmospheric Entry into Jupiter

MICHAEL E. TAUBER*
NASA Ames Research Center, Moffett Field, Calif.

The objectives of this study are to define a near minimum heating shape for a probe designed to enter the atmosphere of Jupiter directly at 50 km/sec. Four atmospheric compositions, pure H_2, 0.6 H_2-0.4 He, 0.4 H_2-0.6 He (by volume), and pure He were considered. Equations for radiative heating, including lines and continua, and convective heating, including effects of mass-addition blockage, were derived. Heating calculations were made for blunt and conical bodies, for lifting and ballistic entry. It is concluded that entries should be made in the direction of planetary rotation, near the equator, at shallow flight-path angles so that heating rates will remain tolerable; advanced heat-shield materials are required; blunt-body heat-shield fractions become large and conical bodies may have to be used; ballistic entries will be difficult with cones so that lifting trajectories (with moderate L/D's) may be required.

Nomenclature

A = base area of entry body
C_1 = constant in Eq. (6b)
C_D = drag coefficient
C_H = surface averaged heat-transfer coefficient
d = maximum diameter of body
D = drag
g = acceleration of gravity
I = radiative specific intensity for given path length
L = lift
m = body mass
p = shock-layer pressure
q = heat transfer into the body up to time t per unit area
Q = heat transfer into the body up to time t
r = radius
Re = boundary-layer-edge Reynolds number
t = time
V_r = flight velocity relative to rotating atmosphere
β = inverse scale height of atmosphere
γ = flight-path angle below horizontal
Γ = radiative cooling parameter
ζ = energy required to ablate unit mass
θ_c = cone half-angle
ρ = freestream density
ρ_s = density in shock layer
σ = asymptotic lower limit of ψ
ψ = ratio of convective heating with ablation to value without ablation

Subscripts

b = body
B = mass-addition parameter
c = convective
E = entry
F = final value
f = face of blunt body
i = initial
l = limiting
max = maximum
min = minimum
N = nose of conical body
OPT = optimum
R = radiative
s = stagnation

Presented as Paper 68-1150 at the AIAA Entry Vehicle Systems and Technology Meeting, Williamsburg, Va., December 3–5, 1968; submitted December 20, 1968; revision received June 23, 1969. The author gratefully acknowledges the aid of his colleagues H. T. Woodward and D. L. Compton in computing the thermodynamic properties of the hydrogen-helium mixtures, and D. M. Cooper and W. J. Borucki in computing the helium line radiation. Also, appreciation is gratefully extended to J. Gaspar for her patient and efficient programing.

* Research Scientist. Associate Fellow AIAA.

Introduction

BECAUSE of their great size and low atmospheric temperature (around 100°K), it is thought that the major planets, especially Jupiter, have maintained their primordial atmospheres to a great extent. In contrast, Earth has lost all its primordial atmosphere and vast ecological changes have altered the composition greatly. Therefore, there is much scientific interest in studying a primitive atmosphere such as that of Jupiter. Entry into Jupiter poses many new and challenging problems because of the high entry speed (up to 60 km/sec) and the unfamiliar composition of its atmosphere.

The presence of methane and ammonia in the Jovian atmosphere was discovered in the 1930's. In 1953, Baum and Code[1] photometrically observed the occultation of the star σ-Arietis by the Jovian atmosphere and determined the atmospheric scale height to be 8.3 km. From this and the mean temperature, they derived a molecular weight of 3.3 with an uncertainty of perhaps as much as ± 1. Since 1960, hydrogen lines have been discovered in the spectrum of Jupiter. In 1962, Öpik[2] proposed a 97% helium-2.3% hydrogen atmosphere. In 1963, Spinard and Trafton[3] and, more recently, Beckman,[4] proposed the atmospheric conditions for Jupiter shown in Table 1. The presence of helium is postulated based on the molecular weight result of Baum and Code. (Neon has not been observed and is included only because of cosmic abundance considerations.[3]) The molecular weights of these mixtures are 3.4 and 2.65, respectively.

The purpose of the preceding brief discussion is to indicate that the best available information on the atmosphere of Jupiter is that it consists predominantly of hydrogen and helium with only trace amounts of heavier gases. Accordingly, only these two light gases will be considered. Atmospheres ranging from pure hydrogen to pure helium, including mixtures of these gases, will be assumed. It is felt that the minor constituents need not be included in computing the thermodynamic environment during entry, especially in view of the lack of specific composition data.

The reader should appreciate that the present knowledge of heat-transfer and heat-shield performance at extreme speeds is subject to considerable uncertainty. Accordingly, the preliminary results presented here should be viewed as indicative of trends rather than as values suitable for final vehicle design.

Analysis

The hyperbolic excess velocities at Jupiter are very small compared to the planet's escape velocity of about 60 km/sec, which, therefore, approximates the velocity for direct entry.

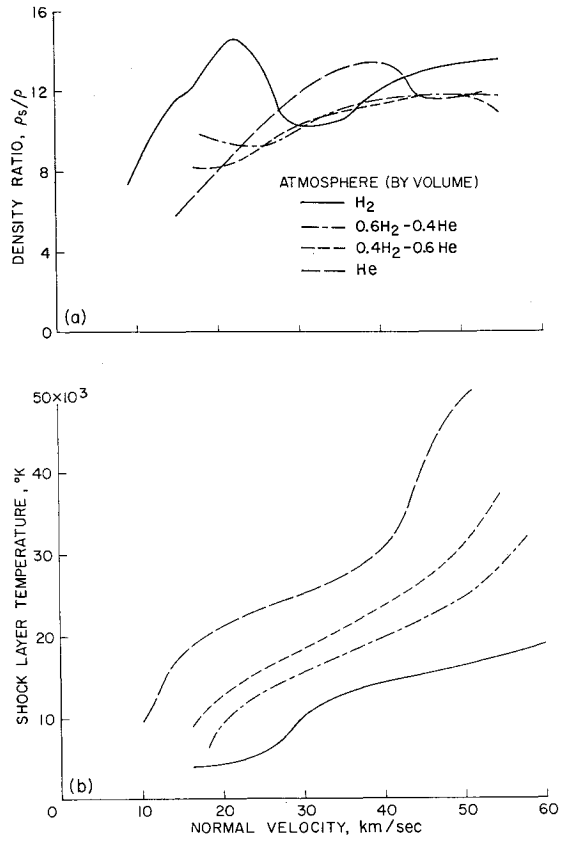

Fig. 1 Shock-layer properties (p = 10 atm); a) density ratio, b) temperature.

However, because of its large size and rapid rotation rate, the equatorial velocity of the planet is about 12.6 km/sec. Therefore, entering in the direction of the planet's rotation and in the vicinity of the equatorial plane can reduce the relative entry speed with respect to the atmosphere, V_{r_E} to about 50 km/sec.

The very high entry velocity will obviously produce severe heating of any entry vehicle, but especially intense shock-layer radiation. Allen et al.[5] have shown that radiation and, therefore, total heat input can be reduced drastically by use of conical rather than blunt entry vehicles. The analysis of Ref. 5 was for ballistic entry and is valid if the body-shape change from ablation is not large. With optimum conical bodies, the heating is primarily convective, and it becomes highly desirable to maintain a laminar boundary layer. The greatly increased heating resulting from turbulent convection can, to a considerable degree, negate the advantage of reduced radiation. Accordingly, Reynolds number limits are imposed on the trajectories studied. Seiff and Tauber[6] extended the work of Ref. 5 to acceleration-limited and Reynolds-number-limited grazing (and hence lifting) entries and also computed the change in nose shape from ablation for cones.

When optimizing vehicles for very intense heating environments, as in the present case, ideally, one should minimize the entire heat-shield weight. However, such an analysis becomes highly complex since mass removal not only by ablation, but also by other mechanisms, should be considered. Also, since the total heat inputs are very high, heat-shield materials with large heats of ablation are needed. This means the heat shield will probably be carbonaceous and, therefore, have a high thermal conductivity, which implies that considerable insulation will be required to protect the payload and structure. Therefore, an analysis treating the entire heat shield is, almost by necessity, limited to one heat-shield material. Such a degree of specialization is felt to be both undesirable and unwarranted at present. Therefore, the following results are based on an optimization of the heat-shield mass loss from ablation. Thus, the only heat-shield properties needed are the intrinsic heat of ablation ζ and the molecular weight of the ablation vapor, since the blockage factor for convective heating, ψ, depends weakly on this property.

Table 1 Atmospheric conditions proposed in Refs. 3 and 4

Gas	Percent by volume[3]	Percent by volume[4]
H_2	60	82
He	36	18
Ne	3	0.2
CH_4, NH_3	<1	0.2

To make the analysis more general, both lifting and ballistic trajectories were used. The lifting trajectory for which results will be given here is the so-called constant Reynolds number descent,[6] a nearly minimum heating trajectory requiring lift modulation.

Stickford and Menard,[7] using the atmospheric composition of Ref. 3, made shock-layer radiation intensity calculations for the vertical ballistic entry into Jupiter of a body having a ballistic coefficient of 310 kg/m^2. For a direct entry, peak radiative intensities ranging from 1000 to 2000 kw/cm^2 sterad were shown for this extreme flight path. Although the importance of nonadiabatic effects was recognized, these were not accounted for and heat transfer to the body was not calculated.

Mass Loss

The equation of motion, tangential to the flight path, is

$$\tfrac{1}{2}\rho V_r^2 C_D A - mg\sin\gamma = -m\,dV_r/dt \tag{1}$$

where V_r is the vehicle velocity relative to the (rotating) atmosphere. During that portion of the entry where heating is important, the drag force is generally much larger than the tangential weight component, and we can write

$$\tfrac{1}{2}\rho V_r^2 C_D A \doteq -m\,dV_r/dt \tag{1a}$$

The heat-transfer rate to the entire body can be written

$$dQ/dt = \tfrac{1}{2}\rho V_r^3 A C_H \tag{2}$$

where C_H is the average heat-transfer coefficient that depends on altitude, velocity, and body geometry. The change of body mass is given by

$$-dm = dQ/\zeta \tag{3}$$

where ζ is defined as the heat absorbed while a unit mass of ablator is brought from the initial to the final state. By combining Eqs. (1–3), we find the mass loss from ablation is

$$dm = (m/\zeta)(C_H/C_D)V_r dV_r \tag{4}$$

or, to find the change in mass during the entire entry,

$$\int_{m_E}^{m_F}\frac{dm}{m} = \int_{V_{r_E}}^{V_{r_F}}\frac{1}{\zeta}\frac{C_H}{C_D}V_r\,dV_r \tag{4a}$$

Integrating and letting

$$m_F = m_E - \Delta m$$

we find the fraction of the mass lost from ablation during entry is

$$\frac{\Delta m}{m_E} = 1 - \exp\left(-\int_{V_{r_F}}^{V_{r_E}}\frac{1}{\zeta}\frac{C_H}{C_D}V_r\,dV_r\right) \tag{5}$$

Heat Transfer

The thermodynamic and transport properties of hydrogen at elevated temperatures were taken from Krascella[8] and Grier,[9,10] respectively, while for helium, Refs. 11 and 12 were used. For the two gas mixtures considered, 60% hydrogen-40% helium and 40% hydrogen-60% helium (by volume), the thermodynamic conditions and species concentrations were computed with an Ames program; the transport properties of these mixtures were calculated by R. S. Devoto of Stanford University, under a contract with Ames Research Center.

The heat-transfer coefficient was written

$$C_H = C_{H_c} + C_{H_R} \tag{6}$$

For the convective contribution, we write

$$C_{H_c} = \frac{1}{\frac{1}{2}\rho V_r^3 A} \int_A \left(\frac{dq}{dt}\right)_{B=0} \psi dA \tag{6a}$$

The convection in hydrogen gas was computed by Marvin and Deiwert.[13] More recently, Ronald Pope of Ames Research Center measured convective heat transfer in helium (to be published). The scaling laws suggested by Marvin and Pope[14] for the blockage effectiveness of the ablation vapors on convective heat transfer were basically used. However, in accordance with ablation tests made at Ames, it is assumed that the convective heating does not go to zero at large mass injection rates, but approaches a finite value σ (here assumed as 0.1) asymptotically. The effect of assuming that total blockage of convection is possible will, however, also be illustrated. From the results of Refs. 13 and 14, we can say that to the level of accuracy of the present analysis

$$C_{H_c} = \frac{C_1}{\frac{1}{2}\rho V_r^3 A} \int_A \left[\left(\frac{dq}{dt}\right)_{B=0}\right]_{\text{air}} \psi \, dA \tag{6b}$$

where C_1 represents the ratio of the heat transfer in a given gas to that in air, and is a function of the molecular weight of the atmospheric gases; the convective heat-transfer rate in air was computed using the method of Ref. 14. Using this approximation, the cold-wall convection ($\psi = 1$) in the gases considered ranges from about 35% of the value for air for hydrogen to about 50% for helium, at the same conditions.

The radiation from hydrogen at high temperatures was computed by Lasher et al.[15] Radiation from high-temperature helium, both line and continuum, for path lengths of 0.1, 1, and 10 cm, was computed as part of the present work. Agreement with the helium radiation calculations of Ref. 16 was very good (within about 20%) at the lower (42.7 km/sec) of the two speeds investigated in Ref. 16; the higher speed was beyond the range considered in the present paper. For mixtures of the two gases, the radiation was computed by scaling the line and continuum components as functions of the composition of the mixture for chosen temperatures and pressures. (A cursory comparison was made between the radiation from the 60% hydrogen-40% helium mixture and the mixture of Ref. 7. Results from the present study had to be extrapolated to the considerably higher shock-layer pressure of Ref. 7, but agreement was generally within about 30%.) The radiative contribution to the heat-transfer coefficient was expressed as

$$C_{H_R} = \frac{1}{\frac{1}{2}\rho V_r^3 A} \int_A \left(\frac{dq}{dt}\right)_R dA \tag{6c}$$

where

$$\left(\frac{dq}{dt}\right)_R = \pi I \times f(\Gamma) \tag{6d}$$

and I is the specific intensity for a given path length. Since the optical properties of the shock layer vary from thin to thick, I was evaluated as a function of twice the path length. (This procedure gives the correct values in the limit for both the thin and thick gases.) Nonadiabatic effects in the shock layer are accounted for by the factor $f(\Gamma)$ which was based on Ref. 17 and written in the form (valid for $\Gamma < 1$)

$$f(\Gamma) = 1/(1 + 4\Gamma^{0.7}) \tag{6e}$$

The calculations of Ref. 17 are for air; however, there is enough similarity between the spectral distribution of energy in air at the conditions of Ref. 17, so that Eq. (6e) should be a reasonable approximation for the gases used here. Self-absorption is important in the present analysis and was also accounted for in Ref. 17, where it was shown that for a given Γ, the effect of radiative cooling is substantially greater than predicted by transparent gas theories.

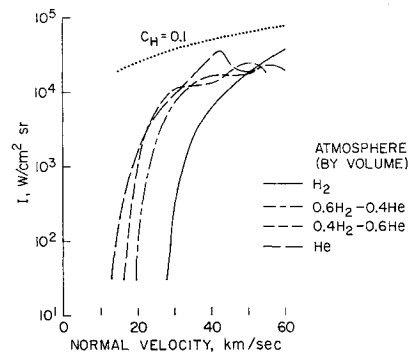

Fig. 2 Radiative intensity from 1-cm-thick isothermal slab for different atmospheric compositions (p = 10 atm).

Results

To illustrate the environment during entry, we will first look briefly at some of the shock-layer properties for the four atmospheric compositions considered. Since radiative heating is so important during these high-speed entries, we will concentrate on those properties that influence the shock-layer radiation. The radiation strongly depends on the shock-layer thickness which, in turn, is inversely proportional to the density ratio. In Fig. 1a the density ratios across a normal shock wave are shown to range between 10 and 14, and are not greatly dependent on composition at high speeds. Next, in Fig. 1b, the shock-layer temperature is shown. Here the effect of atmospheric composition is very strong; in fact, the helium temperatures are from two to three times higher than those for hydrogen, and those for the mixtures fall between. Since hydrogen has strong line and continuum radiation in the ultraviolet portion of the spectrum, this radiation is strongly self-absorbed because of the relatively low temperatures. Therefore, when helium is added to hydrogen, it greatly raises the temperature of the mixture (Fig. 1b), and the hydrogen radiation is substantially increased. In addition, the helium itself is an efficient radiator at high temperatures. The effect is illustrated in Fig. 2, where the radiation from a 1-cm-thick isothermal slab of gas is shown as a function of normal shock velocity for the four assumed atmospheres. The radiation from the hydrogen shock layer is generally much less than from the other compositions except at the highest speed of interest here, 50 km/sec. For comparison, a $C_H = 0.1$ line, that is, heat input equal to $\frac{1}{10}$ of flow energy, is also shown; at this condition, nonadiabatic effects (radiative cooling) become dominant.

Blunt-Body Mass Loss

From Eq. (5) it can be seen that the total mass loss from ablation (which is approximately proportional to the heat input to the body) is inversely proportional to the drag coefficient of the body. It is, therefore, logical to consider

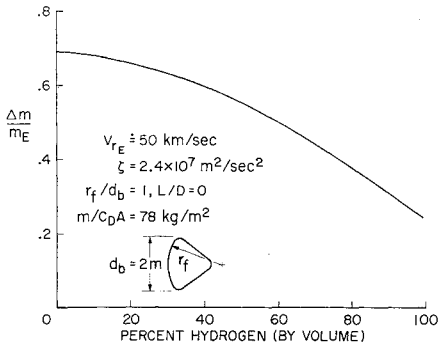

Fig. 3 Mass loss for blunt capsule as a function of atmospheric composition (γ_E = 3.8° at 165 km).

initially a blunt entry body. A shallow ballistic entry is assumed here. As we will see, even for this case the heating rates become very large; for a steep entry the heating rates probably become totally unmanageable. The body selected has a ratio of face radius to maximum diameter of 1 ($C_D \doteq 1.35$). The body has a 2-m diameter† and a ballistic coefficient of 78 kg/m² (0.5 slug/ft²). A vaporizing ablator with intrinsic heat of ablation ζ of 24 million m²/sec² (about 10^4 Btu/lb) was assumed. Since the heating rates are very high, surface reradiation has been neglected to be conservative.

The radiative and convective heating was computed and integrated over the trajectory. The mass-loss ratio as a function of atmospheric composition is shown in Fig. 3 and ranges from about 25 to nearly 70%. Keeping in mind that the total heat-shield mass may exceed by as much as 50% (or possibly more) the mass lost by ablation, we can conclude that the blunt body requires an excessively heavy heat shield over most of the range of atmospheric compositions considered.

Mass Losses of Optimum Conical Bodies

The reduced drag of conical bodies, compared to blunt bodies, must be more than offset by a corresponding reduction in total heat-transfer coefficient in order that they have smaller mass-loss ratios [see Eq. (5)]. As previously mentioned, it is very important to maintain a laminar boundary layer in order to reduce the heating significantly. To this end, boundary-layer-edge Reynolds numbers are limited to values, Re_l, assumed to be the critical Reynolds number for laminar-turbulent transition. Since transition Reynolds numbers on cones are still subject to some uncertainty, three values were chosen: 1 million (for conservatism), 5 million, and 10 million.

The body size, cone angle, and Re_l uniquely define the product of ballistic coefficient, m/C_DA, sine of the flight-path

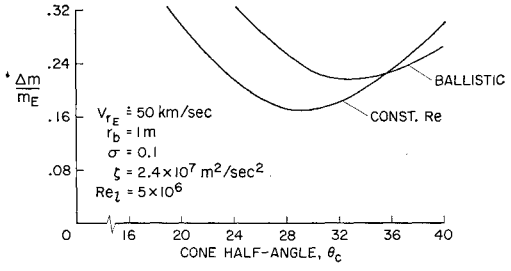

Fig. 4 Variation of mass loss with cone angle for 60% hydrogen-40% helium atmosphere.

† All the bodies considered here have a base area of 3.14 m². The results are insensitive to body size, however, when expressed as mass-loss ratio.

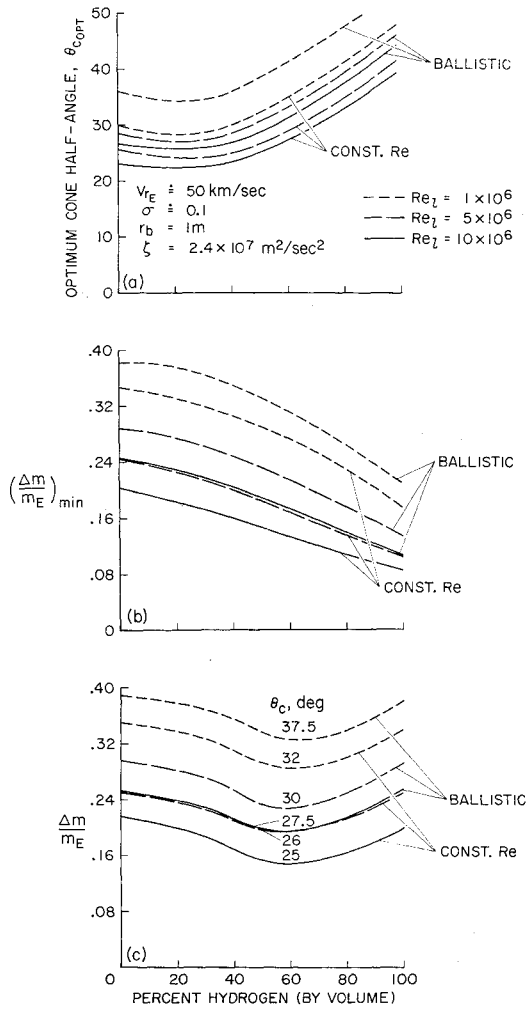

Fig. 5 Effect of atmospheric composition on cones; a) optimum cone half-angles, b) minimum mass-loss ratios, c) mass losses for fixed cone half-angles.

angle, and scale height for ballistic entry, through the relation

$$\frac{m}{C_DA}\beta \sin\gamma = \text{const} \times \left(\frac{Re_l \tan\theta_c}{r_b V_{rE}}\right) \qquad (7)$$

where the constant is 0.53×10^{-5} kg/m sec for H_2 to 2.1×10^{-5} for He. For lifting entry, the body size, cone angle, and Re_l define the combination of L/D and m/C_DA.

By keeping the base area of the cone constant, the mass-loss ratio can be computed as a function of cone angle. Some results are given in Fig. 4 for one atmospheric composition and a Reynolds number limit of 5 million. Figure 4 clearly shows that for each condition there is an optimum cone angle corresponding to a minimum mass-loss ratio. Within ±5° of the optimum angle, the mass losses are not drastically increased; however, at ±10° off the optimum the mass loss may nearly double. The optimum cone half-angles, corresponding to the minimum mass-loss cases, are shown in Fig. 5a and vary from about 20° to 50°, depending on the limit Reynolds number, trajectory, and atmospheric composition. The minimum mass-loss ratios are shown in Fig. 5b as a function of atmospheric composition for three values of the limiting Reynolds number. Note that for the 5 million limit Reynolds number, the mass loss is about half that of the blunt-body case shown in Fig. 3.

From Fig. 5a, we can see that the optimum cone half-angles change by about 20° with atmospheric composition for a given Re_l and trajectory. However, we must keep in mind that the atmospheric composition is assumed unknown in ad-

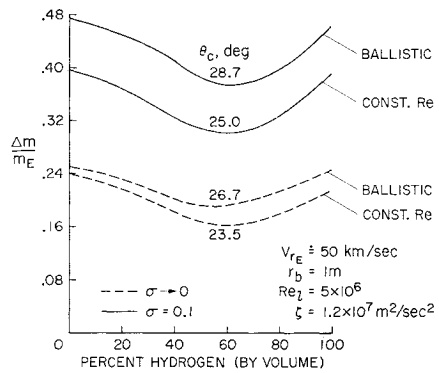

Fig. 6 Mass loss for reduced ablator efficiency.

vance. Thus, at this point, we cannot use the optimum cone angles, but must design for some intermediate fixed value that will achieve the smallest mass loss for the entire range of atmospheres considered. This is shown in Fig. 5c, where the mass-loss variation with atmospheric composition for such a fixed half-cone angle for each trajectory and Reynolds number limit is presented. The mass losses range from 15 to 39% for the two trajectories over the one decade limit Reynolds number range investigated. For a limit Reynolds number of 5 million, the mass losses range from 20 to 30% and corresponding cone half-angles from 26° to 30°.

Effect of Ablator Efficiency on Mass Loss

We will now consider briefly the effect of ablator performance on the mass loss. The intrinsic heat of ablation of 24 million m²/sec² which has been assumed can be expected from advanced materials such as phenolic nylon, for example, if the gases percolating through the char are in thermodynamic equilibrium with the surroundings. If a nonequilibrium state exists, the heat of ablation may be much lower; one-half the equilibrium value will be assumed here (12 million m²/sec²) and applied to entries with a 5 million limit Reynolds number. The results are shown as solid lines in Fig. 6. The mass losses range from 30 to 47%, that is, halving the heat of ablation increases the mass loss by about 50%. (Whether a mass loss of 47% can still be tolerated is questionable; it is certainly very near the upper limit.) Also shown in Fig. 6 is the effect of permitting the convective heating rate to approach zero ($\sigma \to 0$) with sufficiently high mass injection into the boundary layer from ablation caused by radiative heating. This assumption reduces the heat-shield mass lost during entry by 40 to 50%, to values somewhat lower than the equivalent conditions shown in Fig. 5b. Thus, we might hope that the possibly conservative assumption of $\sigma = 0.1$ essentially counteracts what may be an unconservative value for the intrinsic heat of ablation (24 million m²/sec²).

Heating Rates

One of the critical assumptions affecting the results shown so far is that the cone must remain sufficiently sharp at high speeds to maintain the shock-layer characteristics of conical rather than blunt-body flow. Also, the most severe heating encountered by the conical bodies is at the stagnation point, making the protection of the nose region an important problem.

Upon entry, the nose will blunt to a few percent of the cone base radius within a very short time. (The entropy layer caused by this small bluntness is quickly swallowed by the boundary layer, however, and can actually be beneficial in delaying laminar-to-turbulent transition.) Assuming an initial nose radius of 1 cm, the maximum stagnation heating rates and maximum pressures encountered during a shallow ballistic entry are shown as a function of atmospheric composition in

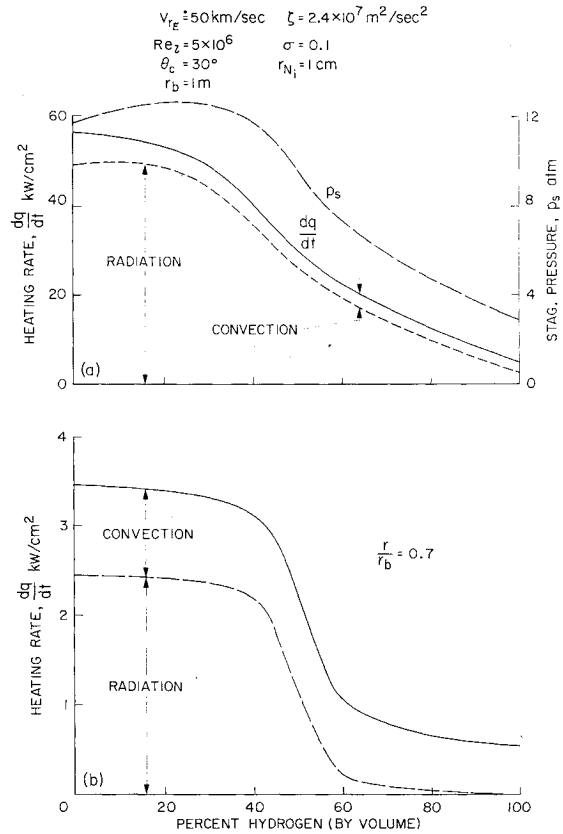

Fig. 7 Maximum heating rates and stagnation pressures for conical body during shallow ballistic entry; a) stagnation point (ablating nose), b) flank (at 0.7 of length point).

Fig. 7a. The heating rates range from about 5 kw/cm² for pure hydrogen to over 50 kw/cm² for pure helium, with shock-layer radiation being the dominant source.‡ At maximum stagnation point heating, the nose radii are in the neighborhood of 10 cm; this value is only weakly dependent on atmospheric composition.

The final nose radii vary, almost linearly, from 0.12 to 0.19 of the cone base radius for hydrogen and helium, respectively, for the conditions shown in Fig. 7a. The duration of the entire entry depends strongly on the atmosphere if we stipulate the same limiting Reynolds number for all compositions; entry into a hydrogen atmosphere takes the longest time and into helium the shortest. Note that the final nose bluntness in the helium atmosphere is only about 50% greater than in

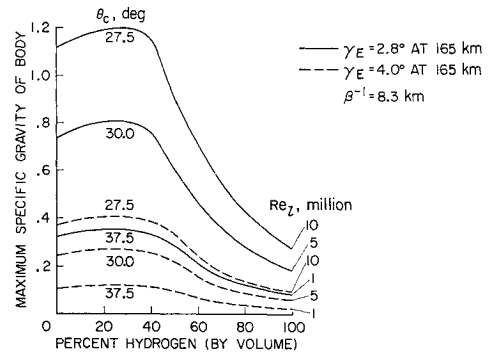

Fig. 8 Maximum allowable specific gravities of bodies.

‡ The curves are general for any combination of $m \sin\gamma/C_D A$ which will observe the Reynolds number limit [see Eq. (7)]. However, as we shall see, the flight-path angle must be shallow for physically realistic bodies.

hydrogen despite the order-of-magnitude difference in the maximum heating rates; this is a direct consequence of the difference in duration of the entries.

The final nose-bluntness ratios corresponding to Fig. 7a are probably not excessive. However, so far it has been tacitly assumed that the ablation occurs in an orderly manner regardless of the magnitude of the heating rate. In reality, it is doubtful whether any known ablator will perform normally at heating rates of 50 kw/cm^2; it is likely that spallation, or other forms of mechanical failure caused by thermal stresses, will account for additional mass removal. An active system, such as film cooling, may, therefore, be required to help protect the cone tip.

In Fig. 7b, the maximum heating rate at the 0.7 flank station on the cone is shown. Note that the rates are lower by an order of magnitude than at the stagnation point and that the convection is a proportionately greater part of the total, being the predominant source of heating in hydrogen-rich atmospheres.

Choice of Trajectory

The mass losses, or total heat inputs, for the shallow (Reynolds number limited) ballistic trajectory are only about 10% higher than for the constant Reynolds number trajectory. The ballistic trajectory is inherently much simpler to fly since it does not require the precise control needed for lift modulation. But, to make a ballistic entry and still observe the Reynolds number limit assumed for maintaining a laminar boundary layer at high speeds requires that the body decelerate rapidly at high altitude. This can be accomplished by requiring a high C_D (incompatible with optimum cone angles found), low mean body density, or a very shallow flight-path angle. The lower limit on the entry-flight-path angle is the value at which atmospheric capture just occurs. For Jupiter, this angle is about 2.8° below horizontal at an altitude of about 165 km above the cloud tops.§ Using this minimum entry angle, the maximum allowable specific gravities of the cones have been calculated and are shown by the solid lines in Fig. 8. It appears that physically realistic body densities are achievable, except for a Re_l of 1 million in the hydrogen-rich atmospheres. Whether we can expect entry-angle guidance accuracies on the order of a fraction of 1°, however, is uncertain. If, instead, we consider an entry angle of 4° and again calculate the maximum allowable body densities, we obtain the values shown by dashed lines in Fig. 8. Now, we find that, except for Re_l greater than about 5 million in helium-rich atmospheres, the allowable vehicle densities become unrealistically low.

We, therefore, turn our attention to the lifting constant Reynolds number trajectory. Calculations were made over the cone half-angle range from 25° to 32° and the limit Reynolds number range from 10^6 to 10^7; for all cases investigated, a maximum L/D of about 0.25 was sufficient to fly such a trajectory to a speed of about 10 km/sec. At this speed, about 95% of the vehicle's kinetic energy at entry has been dissipated.

Concluding Remarks

Many of the results shown in this paper are based on the assumption that the relative proportions of hydrogen and helium in the Jovian atmosphere are unknown and, therefore, cone angles are used here which minimize the mass loss over the entire range of atmospheric compositions. Naturally, this compromises the results achievable with cones of optimum angles, since the optima are dependent on composition. However, if we could even say, with a high level of confidence, that the atmospheric composition falls within a certain range, the mass-losses shown could generally be reduced and, as the range is narrowed, the values achievable with optimum cones can be approached.

One mechanism which could reduce radiative heat transfer to the body significantly, and which was ignored, is the absorption of ultraviolet shock-layer radiation by carbon atoms in the ablation vapor products. This effect was approximately investigated in air in Ref. 18, but the influence of air line radiation was ignored and, therefore, the reduction of radiative heating was substantially overpredicted. A crude effort was made to assess the importance of ablation-product radiation absorption on the results presented here, by fitting a conservative curve to the air data. Using this approach, it was found that blunt-body mass losses might be reduced by 30 to 40% and those for cones by 0 to 20%. Also, conical body stagnation-point heating rates and nose recession may both decrease by 50%. Since the effects may be large, an effort is currently being made to calculate absorption of radiation from a hydrogen-helium shock layer by ablation products.

In summary, the following tentative conclusions have been reached from the present investigation:

1) Entries should be made in the direction of planetary rotation and near the equator to take advantage of Jupiter's high rotational velocity. To take full advantage of this effect, the flight-path angle must be shallow.

2) Shallow flight-path angles are necessary also to keep the heating rates within the realm of manageability; for steep entries, heating rates become so high that the entry could not be made without tremendous improvement in heat-protection materials.

3) Even for shallow entries, heat-shield materials with high intrinsic heats of ablation (24 million m^2/sec^2) are required; theoretically, phenolic nylon is capable of such performance.

4) Blunt-body heat-shield mass-loss fractions will range from 25 to 70% for the pure hydrogen and pure helium atmospheres, respectively.

5) Conical-body heat-shield mass-loss fractions can be kept in the neighborhood of 30% (for all atmospheres considered) if laminar flow can be maintained by limiting boundary-layer-edge Reynolds number to a few million. However, the problem of boundary-layer transition on an ablating surface, correctly simulating roughness, temperature ratio, mass injection rate, etc. requires much more research.

6) We must also improve our understanding of heat-shield performance at high heating rates. For example, the maximum heating rates to be expected on the flank surfaces of the cones are, typically, in the kw/cm^2 regime. Stagnation-point heating rates of about 50 kw/cm^2 can be expected in helium-rich atmospheres; an active cooling system may be needed to protect the nose.

7) Unless an entry-angle guidance accuracy of better than 1° can be achieved, ballistic entries may not be possible with Reynolds number limited conical bodies.

8) An L/D of about 0.25 is sufficient to follow a lifting trajectory, such as a constant Reynolds number descent, to a speed of about 10 km/sec.

9) The large variation in heating rates with atmospheric composition, which is shown in this study, emphasizes the importance and value of improved knowledge of the Jovian atmosphere, which could be gained from a flyby mission.

§ A cloud top pressure of 3 atm has been used here[3] and an inverse scale height of 8.3 km, consistent with the value of Ref. 1.

References

[1] Baum, W. A. and Code, A. D., "A Photometric Observation of the Occulation of σ-Arietis by Jupiter," *Astronomical Journal*, Vol. 58, 1953, p. 108.

[2] Öpik, E. J., "Jupiter: Chemical Composition, Structure, and Origin of a Giant Planet," *Icarus*, Vol. 1, No. 3, Oct. 1962.

[3] Spinrad, H. and Trafton, L. M., "High Dispersion Spectra of the Outer Planets. 1. Jupiter in the Visual and Red," *Icarus*, Vol. 2, No. 1, June 1963.

[4] Beckman, J. E., "The Pressure at the Cloud Top and the Abundance of Hydrogen in the Atmosphere of Jupiter," *Astrophysical Journal*, Vol. 149, No. 2, 1967.

[5] Allen, H. J., Seiff, A., and Winovich, W., "Aerodynamic Heating of Conical Entry Vehicles at Speeds in Excess of Earth Parabolic Speed," TR R-185, 1963, NASA.

[6] Seiff, A. and Tauber, M. E., "Minimization of the Total Heat Input for Manned Vehicles Entering the Earth's Atmosphere at Hyperbolic Speeds," TR R-236, 1966, NASA.

[7] Stickford, C. H. Jr. and Menard, W. A., "Bow Shock Composition and Radiation Intensity Calculations for a Ballistic Entry into the Jovian Atmosphere," AIAA Paper 68-787, Los Angeles, Calif., 1968.

[8] Krascella, N. L., "Tables of the Composition, Opacity, and Thermodynamic Properties of Hydrogen at High Temperatures," SP-3005, 1963, NASA.

[9] Grier, N. T., "Calculation of Transport Properties and Heat-Transfer Parameters of Dissociated Hydrogen," TN D-1406, 1962, NASA.

[10] Grier, N. T., "Calculation of Transport Properties of Ionizing Atomic Hydrogen," TN D-3186, 1966, NASA.

[11] Lick, W. J. and Emmons, H. W., *Thermodynamic Properties of Helium to 50,000°K*, Harvard Univ. Press, Cambridge, Mass., 1962.

[12] Devoto, R. S. and Li, C. P., "Transport Coefficients of Partially Ionized Helium," Rept. SUAAR 291, Dec. 1966, Stanford Univ.

[13] Marvin, J. G. and Deiwert, G. S., "Convective Heat Transfer in Planetary Gases," TR R-224, 1965, NASA.

[14] Marvin, J. G. and Pope, R. N., "Laminar Convective Heating and Ablation in the Mars Atmosphere," *AIAA Journal*, Vol. 5, No. 2, Feb. 1967, pp. 240–248.

[15] Lasher, L. E., Wilson, K. H., and Greif, R., "Radiation from an Isothermal Hydrogen Plasma at Temperatures up to 40,000° K," Rept. 6-76-66-17, revised 1967, Lockheed MSC.

[16] Nelson, H. F. and Goulard, R., "Equilibrium Radiation from Isothermal Hydrogen-Helium Plasmas," *Journal of Quantitative Spectroscopy and Radiative Transfer*, Vol. 8, No. 6, June 1968, pp. 1351–1372.

[17] Page, W. A. et al., "Radiative Transport in Inviscid Nonadiabatic Stagnation-Region Shock Layers," AIAA Paper 68-784, Los Angeles, Calif., 1968.

[18] Coleman, W. D. et al., "Effects of Environmental and Ablator Performance Uncertainties on Heat-Shielding Requirements for Hyperbolic Entry Vehicles," *Journal of Spacecraft and Rockets*, Vol. 5, No. 11, Nov. 1968, pp. 1260–70.

OCTOBER 1969 J. SPACECRAFT VOL. 6, NO. 10

Evaluation of Entry and Terminal Deceleration Systems for Unmanned Martian Landers

EDWIN F. HARRISON* AND TRAVIS H. SLOCUMB JR.†
NASA Langley Research Center, Hampton, Va.

Early unmanned Mars lander vehicles will be severely payload limited due to the low entry vehicle ballistic coefficient, and small launch vehicle (Titan III class) requirements. Since the deceleration systems comprise a major portion of the vehicle weight, a comprehensive study has been performed to minimize the decelerator weights in order to provide a maximum payload capability. Various terminal descent systems were considered with primary emphasis on the parachute-propulsion soft lander, and the parachute-impact attenuator rough lander for out-of-orbit and direct entry with ballistic and lifting entry vehicles. An important phase of the study was the comparison of recent contractural specific design results with the present parametric analysis. The results indicate that the soft lander deceleration systems are lighter than those of the rough lander when conditions of minimum surface density, maximum winds, and surface irregularities are considered. For less severe environmental conditions, the deceleration system weights are competitive.

Nomenclature

a_i = impact deceleration, Earth g's
A = reference area, ft²
C_D = drag coefficient
h = altitude, ft
L/D = lift-drag ratio
M = Mach number
m = entry mass, slug
m/C_DA = ballistic coefficient, slug/ft²
T/W_{σ} = thrust-weight (Mars) ratio
V_e = entry velocity, fps
W = weight, lb
W_{ds} = total deceleration system weight, lb
W_e = entry weight, lb
γ_e = entry angle, deg

Presented as Paper 68-1147 at the AIAA Entry Vehicle Systems and Technology Meeting, Williamsburg, Va., December 3–5, 1968; submitted December 23, 1968; revision received July 22, 1969.

* Aerospace Technologist, Aerophysics Division. Member AIAA.

† Aerospace Technologist, Viking Project Office.

Introduction

EFFORTS to minimize the cost of landing an instrumented payload on the surface of Mars require the consideration of launch vehicles in the Titan III-C class, which imposes severe weight restrictions on the design of the lander vehicle. Furthermore, the tenuous nature of the Martian atmosphere provides a limited aerodynamic retardation capability requiring a large fraction of the vehicle weight for deceleration systems. Particular entry and terminal deceleration systems for Mars missions using the Saturn V launch vehicle have been studied.[1,2] The purpose of the present study is to minimize and compare weights of several candidate deceleration systems so that maximum payload capability can be determined for the Titan III-C class launch vehicle. Primary emphasis was placed on the soft lander that employs a parachute prior to propulsive terminal descent and the rough lander which utilizes a parachute plus an impact attenuator. For these systems, both direct and out-of-orbit ballistic entries were examined as well as direct lifting entry. Other factors considered were entry corridor limitations, atmospheric structure, and surface irregularities. A comparison of the present